

Effect of asymmetry of the radio source distribution on the apparent proper motion kinematic analysis

Oleg Titov¹ and Zinovy Malkin²

¹ Geoscience Australia, GPO Box 378, Canberra, ACT 2601, Australia

² Central Astronomical Observatory at Pulkovo of RAS, Pulkovskoe Ch. 65, St. Petersburg 196140, Russia

Received / Accepted

ABSTRACT

Context. Information on physical characteristics of astrometric radio sources, magnitude and redshift in the first place, is of great importance for many astronomical studies. However, data usually used in radio astrometry is incomplete and often outdated.

Aims. Our purpose is to study the optical characteristics of more than 4000 radio sources observed by the astrometric VLBI technique since 1979. Also we studied an effect of the asymmetry in the distribution of the reference radio sources on the correlation matrices between vector spherical harmonics of the first and second degrees.

Methods. The radio source characteristics were mainly taken from the NASA/IPAC Extragalactic Database (NED). Characteristics of the gravitational lenses were checked with the CfA-Arizona Space Telescope LEns Survey. SIMBAD and HyperLeda databases was also used to clarify the characteristics of some objects. Also we simulated and investigated a list of 4000 radio sources evenly distributed around the celestial sphere. We estimated the correlation matrices between the vector spherical harmonics using the real as well as modelled distribution of the radio sources.

Results. A new list of physical characteristics of 4261 astrometric radio sources, including all 717 ICRF-Ext.2 sources has been compiled. Comparison of our data of optical characteristics with the official International Earth Rotation and Reference Systems Service (IERS) list showed significant discrepancies for about half of 667 common sources. Finally, we found that asymmetry in the radio sources distribution between hemispheres could cause significant correlation between the vector spherical harmonics, especially if the case of sparse distribution of the sources with high redshift. We also identified radio sources having many-year observation history and lack redshift. This sources should be urgently observed at large optical telescopes.

Conclusions. The list of optical characteristics created in this paper is recommended for use as a supplement material for the next International Celestial Reference Frame (ICRF) realization. It can be also effectively used for cosmological studies and planning of observing programs both in radio and optics.

Key words. astrometry – techniques: interferometric – Astronomical data bases: miscellaneous – Cosmology: miscellaneous

1. Introduction

Information on physical characteristics of the astrometric radio sources is important for planning of VLBI experiments and analysis of VLBI data to do a research in cosmology, kinematics of the Universe, etc. In particular, the primary mainspring to this work was a support of the investigation of the systematic effects in apparent motion of the astrometric radio sources observed by VLBI (Gwinn et al. 1997, MacMillan 2005, Titov 2008a, Titov 2008b).

The official list of the physical characteristics of the ICRF radio sources is supported by the IERS (International Earth Rotation and Reference Systems Service) ICRS (International Celestial Reference System) Product Center (Archinal et al. 1997). The latest version of the IERS list is available in the Internet¹. However this list has some deficiencies:

- Not all the sources observed in the framework of geodetic and astrometric experiments are included in the IERS list.
- The characteristics of some sources in the IERS list are outdated or doubtful.

To overcome this problems, we performed a compilation of new list of the physical characteristics of astrometric ra-

dio sources using the latest information. Hereafter this list is referred to as OCARS (Optical Characteristics of Astrometric Radio Sources).

The list of radio sources with their positions was originally taken from the Goddard VLBI astrometric catalogues², version 2007c, with addition of two absent ICRF-Ext.2 (Fey et al. 2004) sources 1039-474 and 1329-665 (**hereafter we will use 8-char IERS designation HHMMsDDd which is an abridged version of the IAU-compliant name 'IERS BHMMsDDd'**). In the last version, the source list was updated using the 2009a_astro.cat catalogue computed by Leonid Petrov³. It gives 4261 radio sources in total.

At this stage mainly the NASA/IPAC Extragalactic Database⁴ (NED) was scoured. Characteristics of the gravitational lenses were checked with the CfA-Arizona Space Telescope LEns Survey⁵ (CASTLES). Several sources were checked with SIMBAD⁶ the HyperLeda⁷ databases. In the OCARS list we have included only the optical characteristics of

² <http://vlbi.gsfc.nasa.gov/solutions/astro>

³ <http://astrogeo.org/vlbi/solutions>

⁴ <http://nedwww.ipac.caltech.edu/>

⁵ <http://cfa-www.harvard.edu/glensdata/>

⁶ <http://simbad.u-strasbg.fr/>

⁷ <http://leda.univ-lyon1.fr/>

Send offprint requests to: Oleg Titov, e-mail: Oleg.Titov@ga.gov.au

¹ http://hpiers.obspm.fr/icrs-pc/info/car_physique_ext1

astrometric radio sources: source type, redshift and visual magnitude. The flux parameters are not included in our list because they are available from other centers directly working on correlation and primary processing of the VLBI observations.

The OCARS was preliminary presented in (Malkin & Titov 2008). In this paper we investigated statistical properties of the list in more detail and study their impact on the kinematic analysis of radio source motions.

Analysis of the radio source apparent motion revealed some statistically significant systematics described by the vector spherical harmonics of the first and second orders (dipole and quadrupole effects, respectively) (Titov 2008a, Titov 2008b). The dipole effect could be caused by the Galactocentric acceleration of the Solar system (Gwinn et al. 1997; Sovers et al. 1998; Kovalevsky 2003; Klioner 2003; Kopeikin & Makarov 2006) or a hypothetical acceleration of the Galaxy relative to the reference quasars. The quadrupole harmonic, considered in details by Kristian & Sachs (1966), could be caused either of the primordial gravitational waves or anisotropic expansion of the Universe. This result was confirmed by Ellis et al. (1985) although they stated “the major problem is that neither the distortion nor the proper motions are likely to be measurable in practice in the foreseeable future”. In this case the quadrupole effect should be redshift-dependent, and the apparent proper motion will increase with redshift. However, Pyne et al. (1996) and Gwinn et al. (1997) also discussed the gravitational waves with the wavelength shorter than the Hubble length. Thus, the proper motion, induced by the short-wavelength gravitational waves, also might be constant over all redshifts.

Due to asymmetry of the astrometric radio source distribution around the sky, the correlation between the vector spherical harmonic components is not zero. Therefore, we studied the effect of the asymmetry using the real uneven and simulated even distribution of the sources.

The OCARS list can be used as a supplement material for the second realization of the International Celestial Reference Frame (ICRF2), as well as a database for kinematic studies of the Universe and other related works, including scheduling of dedicated IVS (International VLBI Service for Geodesy and Astrometry, Schlueter & Behrend 2007) programs.

2. Description of the OCARS

Our primary interest is to get the redshift (z) for astrometric radio sources to develop the previous studies (Gwinn et al. 1997; MacMillan 2005; Titov 2008a, 2008b). In those papers, redshift values were taken from the ICRF list (Archinal et al. 1997). However, as rather tiny effects in the source motions are to be investigated, it is important to increase the number of sources involved in the processing. Searching the latest astrophysical databases, primarily the NED, we could considerably augment the list of astrometric radio sources with known redshift. Nevertheless, more than half of the astrometric radio sources have no determined redshift.

Evidently, the only direct way to get the redshift for other most frequently observed astrometric sources is to organize a dedicated observing program with large optical telescopes. To help in preparation of such a program, we also collect the source type and its visual magnitude if this information is available. Also, it makes a sense to include in this observational program those sources with existing but uncertain redshift values.

It should be noted, that not all astrometric radio sources were reliably identified in the NED. We use the following procedure for identification. In the first step, we search for sources

by source name using “ICRF” and “IVS” prefix. So, we rely on the source identification used in the literature and by the NED staff. Then about 500 sources, mostly from the VCS6 list, were searched by position. We take into account both the angular distance between the VLBI and NED positions as well as their uncertainty in the VLBI and NED positions. For some sources multiply NED objects within the error level were found. For 16 sources no appropriate object was found in the NED, which is mentioned in the comments. The problem of the source identification in the NED and other astrophysical data bases hopefully will be solved after official publication of the VCS6 catalogue.

The OCARS list is made available along with this paper in electronic form.

3. Statistics

The overall statistics of the OCARS is the following.

<u>Number of sources:</u>		
total		4261 (100%)
N	2391 (56.1%)	
S	1870 (43.9%)	
with known type		2545 (59.7%)
AGN	1654 (65.0%)	
galaxy	492 (19.3%)	
star	27 (1.1%)	
other	372 (14.6%)	
with known redshift		1840 (43.2%)
<= 1	853 (46.4%)	
> 1	987 (53.6%)	
N	1195 (64.9%)	
S	645 (35.1%)	
with known visual magnitude		2452 (57.5%)
with known both z and magnitude		1789 (42.0%)
with known z or magnitude		2503 (58.7%)
with known magnitude and unknown z		663 (15.6%)

Figures 1 and 2 show the distribution of the sources with known redshift.

Figure 3 shows the distribution of the visual magnitude. The bottom part of the figure gives an impression about the magnitude of the sources for which redshift is not yet determined.

Therefore, large observational projects for spectroscopy of the astrometric radio sources are very important. Such a program is quite laborious taking into account a necessity of observations of mostly rather weak sources and their careful identification (search for an optical counterpart of radio sources). So, it makes sense to create a list of radio sources which were intensively observed during astrometric and geodetic VLBI programs, and lack of known redshift to establish an order of priority for optical observations. Such a list of high-priority sources is given in Table 1. It was compiled using the IVS observation statistics available at http://www.gao.spb.ru/english/as/ac_vlbi/. The list was sorted using the number of observations marked as good in the observational NGS cards made during 24h sessions (in fact, in sessions of 18 hours and longer). On the other hand, it seems to be reasonable to give a observation priority to sources with reliably determined redshift, especially in the Southern hemisphere, and sources already having a good observational history.

4. Comparison with the IERS list

We have compared the OCARS with the IERS list and found 667 common radio sources. All the sources are present in the

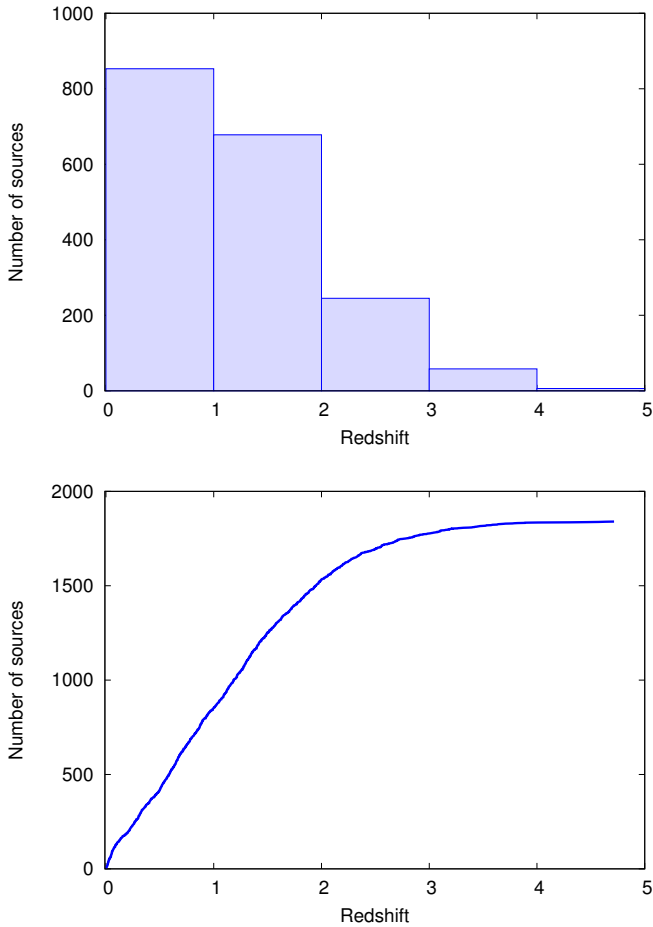


Fig. 1. Distribution of the redshift (*top*) and cumulative number of sources (*bottom*).

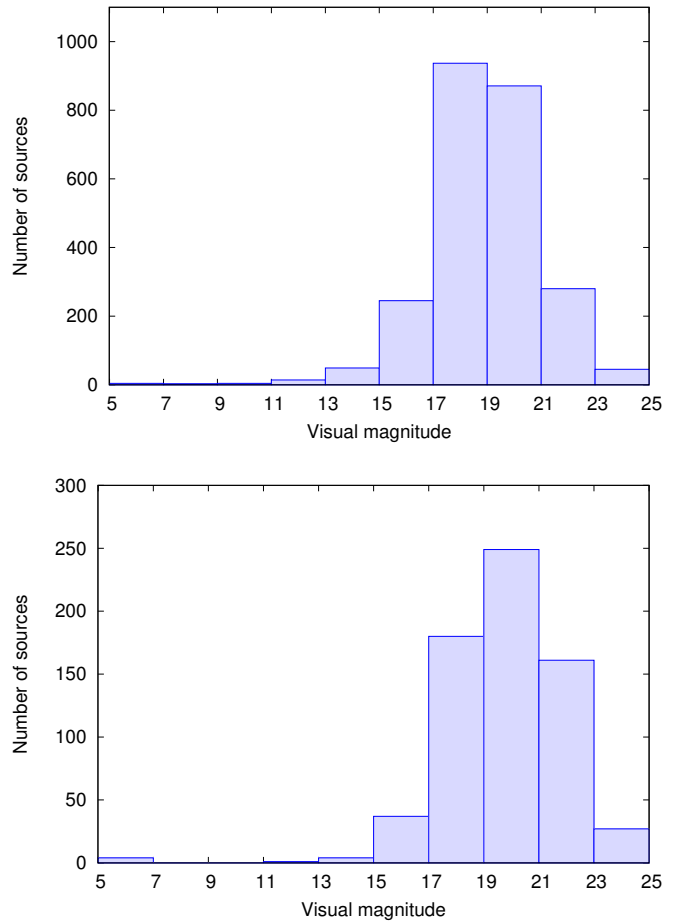


Fig. 3. Distribution of the visual magnitude for all sources (*top*) and for sources without known redshift (*bottom*).

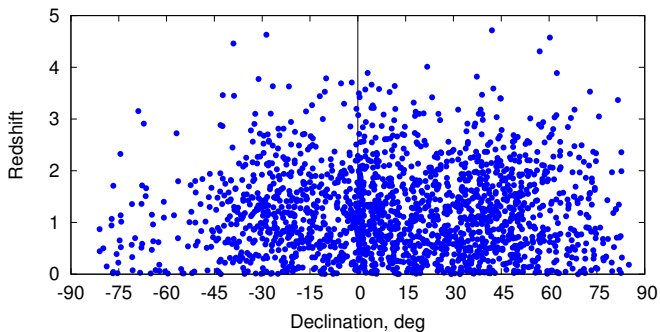


Fig. 2. Distribution of the redshift over declination.

IERS list. Comparison of these two lists results in rather large discrepancy.

- The first evident difference is in the number of radio sources. The OCARS list contains 40 extra ICRF sources plus several hundreds other sources, 4261 vs. 667 objects in total, 2503 vs. 555 objects with known redshift or visual magnitude.
- Unlike the IERS list, we did not try to trace all the details of the Active Galactic Nuclei (AGN) classification that are not always stable and unambiguous. So, all the quasars and BL object are designated as AGN.

- Redshift for 55 more ICRF sources were found; redshift for 4 sources presented in the IERS list were not included in our list for various reasons; for 30 sources redshift differs more than by 0.01; the largest differences are 1.26 (1903-802), 1.20 (1600+431), 0.70 (0646-306).
- Visual magnitudes for 70 more ICRF sources were found; magnitudes for 2 sources were not confirmed in our list; for 195 sources magnitude differs more than by 0.5; the largest differences are 5.2 (1758-651), 5.0 (1156-094, 1322-427), 3.9 (0241+622).

Further investigation has to be made to clarify all found discrepancies between two lists. It should be mentioned that we consider as important and useful for a user to provide a detailed comment in case of doubtful or ambiguous published data.

5. Comparison with the LQAC

We also performed a comparison of the OCARS list with recently published Large Quasar Astrometric Catalogue (LQAC) (Souhay et al. 2009). This catalogue contains information on redshift and luminosity at optical and radio wavelengths for 113666 quasars.

First, it should be noticed that more than one third of the astrometric sources are not quasars (see section 3, hence not all of them are contained in the LQAC. Nevertheless, this comparison seems to be mutually interesting because the information

Table 1. High-priority list of radio sources lacking known redshift.

Source	Nobs	Source	Nobs	Source	Nobs
1357+769	202005	0426+273	994	0017+200	356
1300+580	75748	0019+058	941	0206+136	342
0749+540	67718	1706-174	919	2051+745	337
0718+792	35867	1922-224	908	1651+391	326
0300+470	25613	1746+470	850	0459+135	323
1923+210	25324	2337+264	723	1647-296	313
0735+178	16356	0134+311	708	1243-160	310
0556+238	12553	0826-373	693	0729+259	310
1057-797	6623	0554+242	635	1036+054	310
0656+082	5278	0818-128	633	1951+355	304
2229+695	4759	0458+138	617	0332+078	303
0657+172	4667	0524+034	592	0822+137	301
0454+844	4296	1754+155	567	0602+405	300
1657-261	2735	1823+689	536	1909+161	296
1221+809	2258	1926+087	531	1424+240	293
1929+226	2087	0759+183	530	1734+508	291
2000+472	2086	1656-075	517	0437-454	281
0430+289	2047	1639-062	516	1251-713	277
0648-165	1973	0055-059	509	0743+277	268
0109+224	1954	1604-333	502	0601+245	267
1751+288	1906	1443-162	497	0259+121	263
0420+417	1893	1817-254	490	0951+268	260
2150+173	1789	1327+321	488	0723+219	250
1815-553	1789	2013+163	479	2302+232	248
1459+480	1782	0341+158	472	0613+570	242
0302+625	1660	0415+398	470	0302-623	232
0544+273	1634	0733-174	468	0700-197	226
0920+390	1575	0854-108	453	1433+304	225
0159+723	1508	1602-115	447	1830+139	222
0440+345	1467	0854+213	446	1705+135	215
1738+476	1413	1922+155	438	0629+160	215
2021+317	1335	1947+079	435	1013+127	215
1307+121	1296	2000+148	433	0728+249	214
1213-172	1285	0115-214	424	0025+197	213
0308-611	1280	1101-536	405	1344+188	205
0722+145	1269	1409+218	400	1451+270	200
0506+101	1233	0912+297	397	0516-621	200
1932+204	1128	0627-199	376	1156-094	198
0039+230	1123	0530-727	375	1412-368	196
2030+547	1056	0725+219	369	0627+176	195

Table 2. Statistics of comparison of OCARS (1) with LQAC (2).

Number of sources ...	Search radius, arcsec				
	1	2	5	10	30
not found in (2)	669	650	641	635	631
without z in both catalogues	1809	1811	1814	1817	1821
with z in (1) only	547	548	532	526	520
with z in (2) only	8	8	8	10	10
with different z in (1) and (2)	44	48	47	47	50

sources used to compile both lists evidently have a large intersection, but are not fully the same. Also, such a check allows us to reveal possible mistakes, overlooked literature, etc.

Since LQAC has no source names, the source identification was made using their position in both catalogues, which corresponds to the method used by the authors of LQAC. Table 2 show a summary of comparison results for five 5 different search radii. Here we compared only redshift values as the most important parameter. The redshift difference of 0.01 was used to detect the significant redshift difference between two compared catalogues.

The most interesting result to us are sources having redshift in the LQAC and lack it in the OCARS. Those sources are 0003-302, 0118-283, 1026-084, 1202+527, 1225+028, 1332+031, 1422+231, 1555+030, 1639-062, and 2256-084. The first analysis showed that the sources 0003-302 and 1026-084 are located in very populated sky region, and maybe more careful identification is needed. The redshift value for the former is referred to a private communication. The source 1422+231 is a component of a gravitational lens according to CASTLES. These and other discrepancies found during this comparison will be analyzed during preparation of the next OCARS version.

An interesting point is the number of the OCARS objects not found in the LQAC. One can see that about 85% OCARS objects were found in the LQAC, which is much greater than the number of OCARS object with known type. On the other hand, the number of the OCARS objects not found in the LQAC is less than the number of OCARS non-AGN objects. It may be worth re-visiting the object classification in both catalogues, in fact in LQAC and NED. Such a large work is out of the scope of this study however.

6. Vector spherical functions

The paucity of the radio sources with declination less than -30° (Fig 2) may result in difficulties for astrometric analysis of radio catalogues. A worse precision of the radio source coordinates in the Southern hemisphere has been reported in papers on the International Celestial Reference Frame (Ma et al. 1998). It may cause more dramatic impact on the analysis of the apparent proper motion of the reference radio sources.

The ICRF consists of a set of highly accurate positions of reference radio sources as determined by the VLBI techniques. The observed radio sources are very distant, therefore when the ICRF is made, their physical proper motion is assumed to be negligible (less than $1 \mu\text{as}/\text{year}$) and their positions are practically stable. However, the motion of relativistic jets from the active extragalactic nuclei can mimic the proper motion of the observed radio sources (with a magnitude up to $0.5 \text{ mas}/\text{yr}$) (see e.g. Marcaide et al. 1985; Alberdi et al. 1993; Fey et al. 1997; Feissel-Vernier 2003; Titov 2007; MacMillan & Ma 2007). Moreover, some tiny systematic effects (dipole and quadrupole) in the apparent proper motion have been observed (Titov 2008a, 2008b). A study of these apparent proper motion would become an important part of the future fundamental reference frame making up.

The dipole and quadrupole systematic effect in the radio source apparent motion were studied previously (Gwinn et al. 1997; MacMillan 2005; Titov 2008a, 2008b) using the expansion of the apparent motion field on vector spherical harmonics. Unfortunately, due to uneven distribution of the reference radio sources over the sky the results could be corrupted by the correlation between estimated parameters. However, the correlation matrices have not been studied carefully so far.

The vector spherical harmonics Hill (1954) are used to study the systematic effect in a proper motion of celestial objects (see e.g. Mignard & Morando 1990; Gwinn et al. 1997; Vityazev & Shuksto 2004; Vityazev & Tsvetkov 2009).

Let us consider $F(\alpha, \delta)$ as a vector field of a sphere described by the components of the apparent proper motion vector $(\mu_\alpha \cos \delta, \mu_\delta)$

$$F(\alpha, \delta) = \mu_\alpha \cos \delta \mathbf{e}_\alpha + \mu_\delta \mathbf{e}_\delta, \quad (1)$$

Table 3. Statistic of the model and real distributions of the radio sources over four redshift intervals. The number of radio sources and the maximum correlation between the thirteen estimated parameters are shown.

Zone	Model		Real	
	N	Max corr	N	Max corr
$0 < z < 1$	1431	0.15	835	0.27
$1 < z < 2$	1183	0.15	671	0.33
$2 < z < 3$	398	0.18	240	0.34
$3 < z < 4$	100	0.19	57	0.51

where $\mathbf{e}_\alpha, \mathbf{e}_\delta$ — unit vectors. A vector field of spherical functions $\mathbf{F}(\alpha, \delta)$ can be approximated by the vector spherical functions as follows

$$\mathbf{F}(\alpha, \delta) = \sum_{l=1}^{\infty} \sum_{m=-l}^l (a_{l,m}^E \mathbf{Y}_{l,m}^E + a_{l,m}^M \mathbf{Y}_{l,m}^M), \quad (2)$$

where $\mathbf{Y}_{l,m}^E, \mathbf{Y}_{l,m}^M$ — the ‘electric’ and ‘magnetic’ transverse vector spherical functions, respectively:

$$\begin{aligned} \mathbf{Y}_{l,m}^E &= \frac{1}{\sqrt{l(l+1)}} \left(\frac{\partial V_{l,m}(\alpha, \delta)}{\partial \alpha \cos \delta} \mathbf{e}_\alpha + \frac{\partial V_{l,m}(\alpha, \delta)}{\partial \delta} \mathbf{e}_\delta \right), \\ \mathbf{Y}_{l,m}^M &= \frac{1}{\sqrt{l(l+1)}} \left(\frac{\partial V_{l,m}(\alpha, \delta)}{\partial \delta} \mathbf{e}_\alpha - \frac{\partial V_{l,m}(\alpha, \delta)}{\partial \alpha \cos \delta} \mathbf{e}_\delta \right). \end{aligned} \quad (3)$$

The function $V_{l,m}(\alpha, \delta)$ is given by

$$V_{l,m}(\alpha, \delta) = (-1)^m \sqrt{\frac{(2l+1)(l-m)!}{4\pi(l+m)!}} P_l^m(\sin \delta) \exp(im\alpha), \quad (4)$$

where $P_l^m(\sin \delta)$ — the associated Legendre functions

The coefficients of expansion $a_{l,m}^E, a_{l,m}^M$ to be estimated as follows

$$\begin{aligned} a_{l,m}^E &= \int_0^{2\pi} \int_{-\frac{\pi}{2}}^{\frac{\pi}{2}} \mathbf{F}(\alpha, \delta) \mathbf{Y}_{l,m}^{E*}(\alpha, \delta) \cos \delta \, d\alpha \, d\delta, \\ a_{l,m}^M &= \int_0^{2\pi} \int_{-\frac{\pi}{2}}^{\frac{\pi}{2}} \mathbf{F}(\alpha, \delta) \mathbf{Y}_{l,m}^{M*}(\alpha, \delta) \cos \delta \, d\alpha \, d\delta, \end{aligned} \quad (5)$$

where * means a complex conjugation. This system of equations can be solved by the least squares method. In this research the coefficients are estimated as global parameters from a large set of VLBI data.

The three ‘electric’ spherical harmonics for $l=1$ produces the dipole effect corresponding to the acceleration of the Solar system. The three $l=1$ ‘magnetic’ harmonics describe a rotation of the set of quasars. This rotation is not separable from the Earth’s rotation, and, therefore, not estimated. The five $l=2$ ‘electric’ spherical harmonics correspond either to the gravitational waves or to the Universe anisotropic expansion, and, finally, the five $l=2$ ‘magnetic’ spherical harmonics correspond only to the gravitational waves. In total, 13 components are to be estimated.

We studied both real and modelled distributions of the radio sources to calculate the correlations between the spherical harmonics (see Fig 4). For modelling, we initially created a set of 4000 radio sources uniformly distributed over the sky. Then we assigned redshift to all simulated objects in a such way that the redshift values have the same distribution as real ones. Another model set of sources was created from the first one by thinning of the sources within $\pm 15^\circ$ zone along the Galactic equator, to get an ‘avoidance zone’ similar to the real distribution. These distributions are shown in Fig 4.

A comparison of the correlation matrices corresponding to two modelled distribution shown in Fig 4 highlights that the avoidance zone increases the maximum correlation (in absolute values) between the estimated spherical harmonics from 0.03 to 0.16. It is obvious that the paucity of the radio sources under declination -30° (for the real distribution) results in further increase of the correlation to the maximum absolute value 0.28.

Once the separation on different zones on redshift is applicable, we also considered the correlation between observables in four zones for the both model and real distribution (Figs. 5 and 6, respectively). The model distribution without essential decrease in the number of sources around the South Celestial Pole produces almost equal maximum correlation parameter for all four redshift zones (from 0.15 to 0.19)

In opposite, a deficit of the radio sources around the South Celestial Pole is more crucial. The data presented in Figs. 6 demonstrate the impact of the North-South asymmetry in the real distribution of the radio sources. For the zone of redshift between 3 and 4 the maximum correlation reaches 0.51.

As we learnt from the comparison of correlation matrices for the limited number of radio sources unevenly distributed around the celestial sphere, the correlation between estimated spherical harmonics might increase dramatically to level of 0.8–0.9, especially if not all the sources are observed. Whereas, the individual apparent motion due to intrinsic structure reaches $500 \mu\text{as/yr}$ (Feissel-Vernier 2003; MacMillan & Ma 2007; Titov 2007), they could propagate systematically to the estimated parameters, if the number of objects is not sufficient, i.e. for the case of high redshift.

7. Conclusion

To conclude, it is necessary to note that this ‘historic’ deficit of the radio sources (and, additionally, the radio sources with measured redshift) might cause problems with further investigation of the hardly detectable systematic effects in the proper motion of the reference radio sources. Therefore, large observational projects for spectroscopy of the astrometric radio sources in the Southern hemisphere are very important. Nonetheless, some observations in the North hemisphere also need to be undertaken.

Independently, the MASIV scintillation survey (Lovell et al. 2003, 2009) also demonstrates a highly significant dramatic decrease in the numbers of scintillators for redshifts in excess of $z = 2$. The lack of scintillation at high redshifts is clear evidence for an increase in the source angular sizes with increasing redshift. Such an increase may be cosmological in origin or may be a propagation effect of inter-galactic scattering (Lovell et al. 2009).

To observe and study radio source in both frequency range (optical and radio) characteristics such as visual magnitude, redshift in optic and flux density in several radio bands have to be measured. We also need to be sure that the same source is observed by the optical and radio instruments. Due to possible misalignment between optical and radio positions the physical characteristics might help to solve the problem of identification.

To chase this aim, a new list of optical characteristics of 4261 astrometric radio sources, OCARS, including all 717 ICRF-Ext.2 sources has been compiled. The OCARS list includes source type, redshift and visual magnitude (when available). Detailed comments are provided when necessary, which is especially useful in understanding of incomplete, contradictory and controversial astrophysical data. The OCARS may serve to various VLBI tasks, for instance:

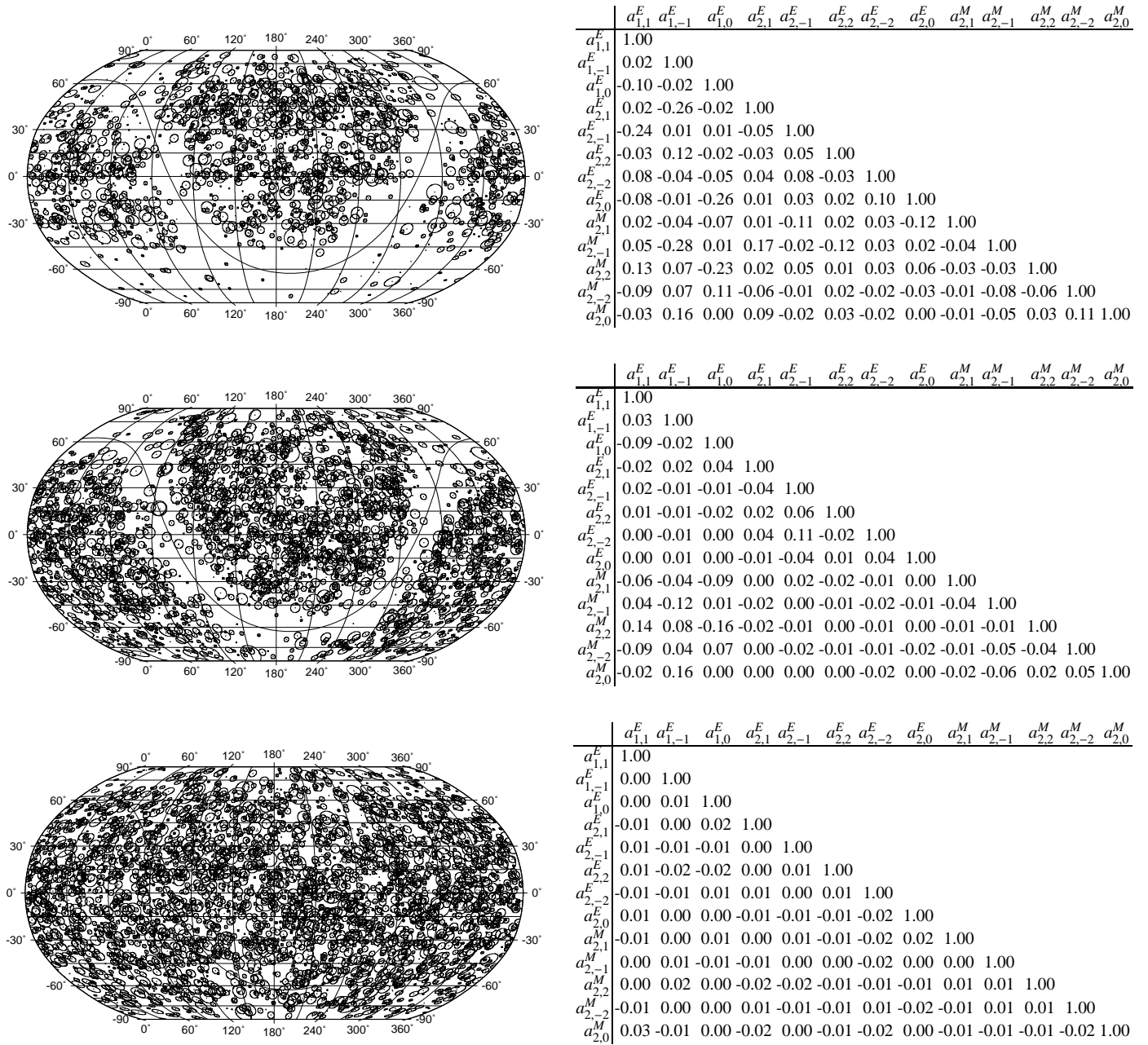


Fig. 4. Sky coverage and correlation matrix for 13 vector spherical harmonics of first and second order for real source distribution of the 1809 radio sources with known redshift for real distribution (*top*) and two modelled distributions of 3123 radio source with the avoidance zone (*middle*) and of 4000 radio sources without the avoidance zone (*bottom*). The circle size corresponds to the redshift value.

- As a supplement material for the second ICRF realization ICRF2 (Ma 2008).
- As a database for VLBI data analysis.
- For planning of IVS and other observing programs, in order to enrich the observational history of the sources with reliable determined redshift.
- For future link between optical (GAIA) and radio (ICRF) celestial reference frames, once the GAIA optical position of about 100,000 quasars will be available.

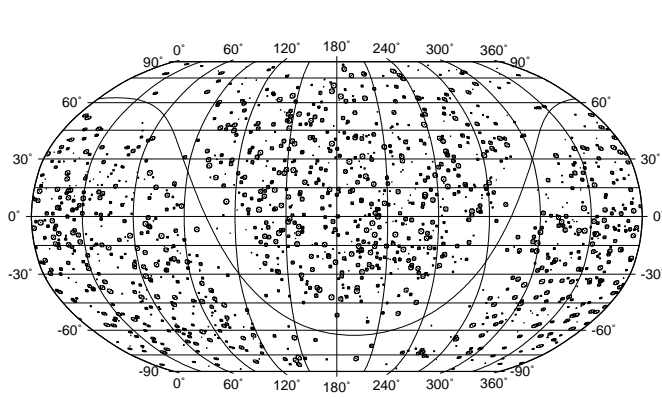
We performed a detailed comparison of the OCARS list with the official IERS list, and found many discrepancies for about a half of common sources. This comparison showed that the IERS list seems to be outdated and should be used with care. Besides, the IERS list, being intended to provide physical characteristics

of the IERS sources only, contains only a small fraction of the whole set of astrometric radio sources used nowadays.

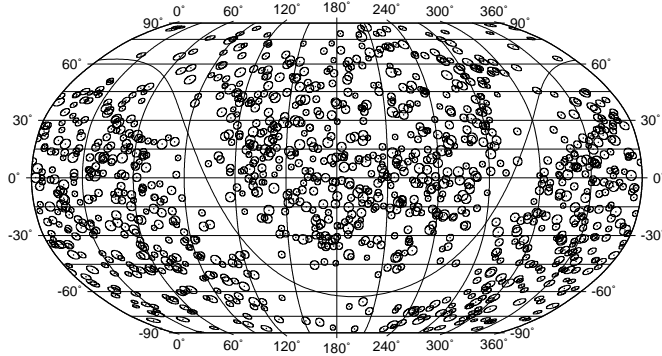
We also compared the OCARS with the newest Large Quasar Astrometric Catalogue LQAC, and found discrepancies which worth further investigating. Most of discrepancies seems to be a result of different object identification.

This is only the first stage of our work. We are planning the following steps:

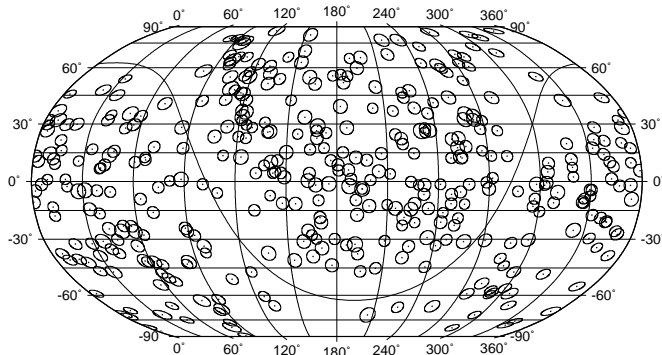
- To continue searching for the missing and checking out the ambiguous characteristics through literature and astronomical databases.
- To organize photometric and spectroscopy observations of astrometric radio sources with large optical telescopes. In particular, such an observational program started at Pulkovo



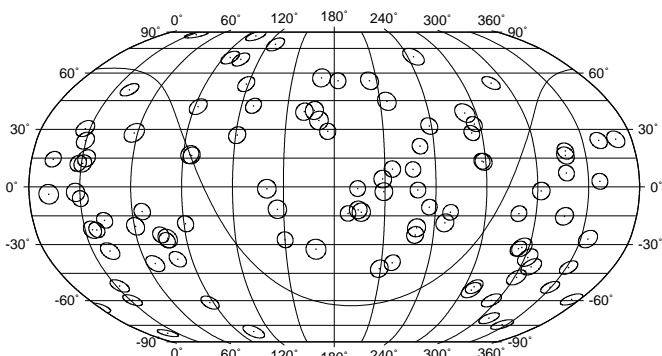
	$a_{1,1}^E$	$a_{1,-1}^E$	$a_{1,0}^E$	$a_{2,1}^E$	$a_{2,-1}^E$	$a_{2,2}^E$	$a_{2,-2}^E$	$a_{2,0}^E$	$a_{2,1}^M$	$a_{2,-1}^M$	$a_{2,2}^M$	$a_{2,-2}^M$	$a_{2,0}^M$
$a_{1,1}^E$	1.00												
$a_{1,-1}^E$	0.03	1.00											
$a_{1,0}^E$	-0.10	-0.04	1.00										
$a_{2,1}^E$	-0.01	0.04	0.03	1.00									
$a_{2,-1}^E$	0.03	-0.01	-0.01	-0.04	1.00								
$a_{2,2}^E$	-0.01	-0.01	-0.01	0.03	0.08	1.00							
$a_{2,-2}^E$	0.02	0.00	0.00	0.04	0.10	0.00	1.00						
$a_{2,0}^E$	0.00	0.02	0.03	-0.01	-0.03	0.00	0.07	1.00					
$a_{2,1}^M$	-0.07	-0.04	-0.09	0.00	0.01	0.00	-0.02	-0.01	1.00				
$a_{2,-1}^M$	0.04	-0.15	0.04	-0.02	0.00	-0.02	-0.04	-0.02	-0.04	1.00			
$a_{2,2}^M$	0.13	0.09	-0.19	0.00	-0.01	0.00	0.00	0.00	-0.02	-0.03	1.00		
$a_{2,-2}^M$	-0.12	0.03	0.07	-0.01	-0.01	0.00	-0.01	-0.01	0.00	-0.05	-0.03	1.00	
$a_{2,0}^M$	-0.06	0.17	0.00	0.01	0.02	0.01	-0.01	0.00	-0.02	-0.06	0.01	0.09	1.00



	$a_{1,1}^E$	$a_{1,-1}^E$	$a_{1,0}^E$	$a_{2,1}^E$	$a_{2,-1}^E$	$a_{2,2}^E$	$a_{2,-2}^E$	$a_{2,0}^E$	$a_{2,1}^M$	$a_{2,-1}^M$	$a_{2,2}^M$	$a_{2,-2}^M$	$a_{2,0}^M$
$a_{1,1}^E$	1.00												
$a_{1,-1}^E$	0.03	1.00											
$a_{1,0}^E$	-0.09	-0.01	1.00										
$a_{2,1}^E$	-0.01	0.02	0.03	1.00									
$a_{2,-1}^E$	0.03	-0.02	-0.02	-0.03	1.00								
$a_{2,2}^E$	0.03	-0.03	-0.02	0.01	0.06	1.00							
$a_{2,-2}^E$	-0.02	-0.03	0.01	0.04	0.10	-0.03	1.00						
$a_{2,0}^E$	0.02	-0.02	-0.01	-0.02	-0.03	0.00	0.03	1.00					
$a_{2,1}^M$	-0.06	-0.03	-0.08	0.00	0.04	0.00	-0.01	0.02	1.00				
$a_{2,-1}^M$	0.03	-0.11	0.00	-0.04	0.00	0.00	0.01	0.02	-0.03	1.00			
$a_{2,2}^M$	0.13	0.08	-0.15	-0.02	-0.02	0.00	-0.03	0.00	-0.01	-0.01	1.00		
$a_{2,-2}^M$	-0.09	0.04	0.07	0.01	-0.03	-0.03	0.01	-0.02	-0.02	-0.04	-0.05	1.00	
$a_{2,0}^M$	0.00	0.15	0.00	-0.02	-0.03	-0.01	-0.02	0.00	-0.02	-0.06	0.02	0.04	1.00



	$a_{1,1}^E$	$a_{1,-1}^E$	$a_{1,0}^E$	$a_{2,1}^E$	$a_{2,-1}^E$	$a_{2,2}^E$	$a_{2,-2}^E$	$a_{2,0}^E$	$a_{2,1}^M$	$a_{2,-1}^M$	$a_{2,2}^M$	$a_{2,-2}^M$	$a_{2,0}^M$
$a_{1,1}^E$	1.00												
$a_{1,-1}^E$	0.04	1.00											
$a_{1,0}^E$	-0.09	0.01	1.00										
$a_{2,1}^E$	-0.05	-0.06	0.08	1.00									
$a_{2,-1}^E$	-0.06	-0.02	-0.01	-0.01	1.00								
$a_{2,2}^E$	0.01	0.01	-0.06	-0.01	0.02	1.00							
$a_{2,-2}^E$	0.02	0.02	-0.01	0.03	0.13	-0.04	1.00						
$a_{2,0}^E$	-0.01	0.05	-0.08	-0.02	-0.05	0.06	-0.02	1.00					
$a_{2,1}^M$	-0.05	-0.04	-0.07	0.00	-0.03	-0.09	-0.03	-0.02	1.00				
$a_{2,-1}^M$	0.04	-0.09	-0.01	0.03	0.00	-0.07	-0.02	-0.06	0.00	1.00			
$a_{2,2}^M$	0.18	0.04	-0.13	-0.04	0.00	0.03	0.03	0.02	0.02	0.02	1.00		
$a_{2,-2}^M$	-0.03	0.09	0.08	0.00	0.00	0.02	-0.02	-0.06	-0.01	-0.06	-0.05	1.00	
$a_{2,0}^M$	0.03	0.15	-0.01	0.01	0.04	0.02	-0.05	0.01	-0.02	-0.06	0.06	0.00	1.00



	$a_{1,1}^E$	$a_{1,-1}^E$	$a_{1,0}^E$	$a_{2,1}^E$	$a_{2,-1}^E$	$a_{2,2}^E$	$a_{2,-2}^E$	$a_{2,0}^E$	$a_{2,1}^M$	$a_{2,-1}^M$	$a_{2,2}^M$	$a_{2,-2}^M$	$a_{2,0}^M$
$a_{1,1}^E$	1.00												
$a_{1,-1}^E$	0.11	1.00											
$a_{1,0}^E$	-0.11	0.03	1.00										
$a_{2,1}^E$	-0.04	-0.03	0.09	1.00									
$a_{2,-1}^E$	0.03	-0.03	-0.05	-0.11	1.00								
$a_{2,2}^E$	0.04	-0.04	0.00	0.03	0.00	1.00							
$a_{2,-2}^E$	-0.06	-0.06	0.04	0.08	0.19	0.01	1.00						
$a_{2,0}^E$	0.02	-0.02	0.06	0.09	-0.14	0.02	-0.08	1.00					
$a_{2,1}^M$	0.00	-0.09	-0.11	0.00	-0.01	-0.02	0.06	0.04	1.00				
$a_{2,-1}^M$	0.10	-0.03	-0.03	0.03	0.00	0.09	-0.05	0.02	-0.12	1.00			
$a_{2,2}^M$	0.19	0.11	-0.03	-0.05	-0.03	0.01	0.07	-0.06	0.01	-0.01	1.00		
$a_{2,-2}^M$	-0.07	0.07	0.18	0.03	-0.06	0.09	-0.01	0.00	-0.03	-0.01	0.01	1.00	
$a_{2,0}^M$	0.08	0.21	-0.02	-0.06	-0.02	-0.09	-0.03	-0.01	0.07	-0.13	0.06	-0.05	1.00

Fig. 5. Sky coverage and correlation matrix for 13 vector spherical harmonics of first and second order for modelled source distribution and four redshift intervals. From top to bottom: $0 < z < 1$, $1 < z < 2$, $2 < z < 3$, $3 < z < 4$. The circle size corresponds to the redshift value.

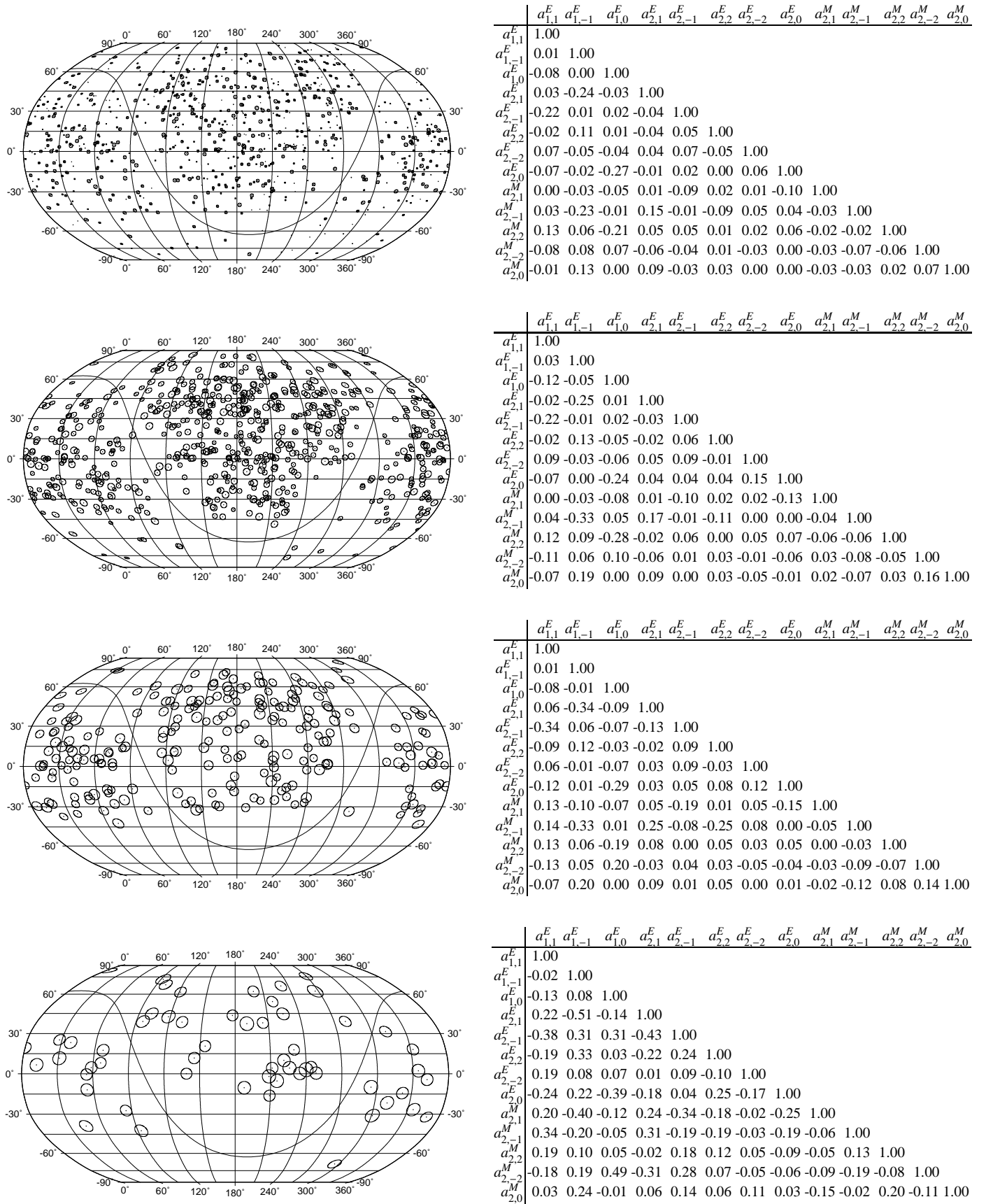


Fig. 6. Sky coverage and correlation matrix for 13 vector spherical harmonics of first and second order for real source distribution and four redshift intervals. From top to bottom: $0 < z < 1$, $1 < z < 2$, $2 < z < 3$, $3 < z < 4$. The circle size corresponds to the redshift value.

Observatory in 2008. Observations are being made on the 6-m BTA telescope of the Special Astrophysical Observatory in North Caucasus.

The list of optical characteristics of astrometric radio sources presented in this paper is publicly available at www.gao.spb.ru/english/as/ac_vlbi/sou_car.dat and is updated once in several months.

Acknowledgements

This research has made use of the NASA/IPAC Extragalactic Database (NED) which is operated by the Jet Propulsion Laboratory, California Institute of Technology, under contract with the National Aeronautics and Space Administration, the SIMBAD and HyperLeda databases, and the CfA-Arizona Space Telescope Lens Survey (CASTLES). Valuable comments and suggestions of the anonymous reviewer are highly appreciated.

References

- Alberdi, A., Marcaide, A., Marscher, A., et al. 1993, *AJ*, 402, 160
 Archinal, B. A., Arias, E. F., Gontier, A.-M., & Mercuri-Moreau, C. 1997, *IERS Technical Notes No. 23*, III-11
 Ellis, G. F. R., Nel, S., D., Maartens, R., et al. 1985, *Phys. Rep.*, 124, 315
 Feissel-Vernier, M. 2003, *A&A*, 403, 105
 Fey, A. L., Eubanks, T.M., & Kingham, K., 1997, *AJ*, 114, 2284
 Fey, A. L., Ma, C., Arias, E. F., et al. 2004, *AJ*, 127, 3587
 Gwinn, C. R., Eubanks, T. M., Pyne T., et al. 1997, *ApJ*, 485, 87
 Hill, E.L. 1954, *Am J Phys*, 22, 211
 Klioner, S. 2003, *AJ*, 125, 1580
 Kopeikin, S. M. Makarov, V. V. 2006, *AJ*, 131, 1471
 Kovalevsky, J. 2003, *A&A* 404, 743
 Kristian, J., & Sachs, R. K. 1966, *ApJ*, 143, 379
 Lovell, J. E. J., Jauncey, D. L., Bignall, H. E., et al. 2003, *AJ*, 126, 1699
 Lovell, J. E. J., Rickett, B. J., Macquart, J.-P., et al. 2009, *ApJ*, 689, 108
 Ma, C., Arias, E., Eubanks, T.M, et al. 1998, *AJ*, 116, 516
 Ma, C. 2008, in: *The Celestial Reference Frame for the Future*, Proc. Journées 2007, ed. N. Capitain, 3
 Macmillan, D. S. 2005, in: *ASP Conference Proceedings*, 340, ed. J. Romney, & M. Reid, 477
 MacMillan, D., & Ma, C. 2007, *JoG*, 81, 443
 Malkin, Z., & Titov, O. 2008, in *Measuring the Future*, Proc. 5th IVS General Meeting, ed. A. Finkelstein, & D. Behrend, 183
 Marcaide, J., Bartel, N., Gorenstein, M., et al. 1985, *Nature*, 314, 424
 Mignard, F., & Morando, B. 1990, in *Proc. Colloque André Danjon*, Journées 1990, ed. N. Capitaine, & S. Débarbat, 151
 Pyne, T., Gwinn, C. R., Birkinshaw, M., et al. 1996, *ApJ*, 465, 566
 Schlüter, W., & Behrend, D. 2007, *J. Geod.*, 81, 479
 Souchay J., Andrei A.H., Barache C., et al. 2009, *A&A*, 494, 799
 Sovers, O. J., Fanselow J. L., & Jacobs C. S. 1998, *Rev. Mod. Phys.*, 70, 1393
 Titov, O. 2007, *Astronomy Letters*, 33, 481
 Titov, O. 2008a, in: *The Celestial Reference Frame for the Future*, Proc. Journées 2007, ed. N. Capitain, 16
 Titov, O. 2008b, in: *Measuring the Future*, Proc. 5th IVS General Meeting, ed. A. Finkelstein, & D. Behrend, 265
 Vityazev, V., & Shuksto, A. 2004, *ASP Conf. Ser.*, 316, 230
 Vityazev, V. V., & Tsvetkov, A. S. 2009, *Astronomy Letters*, 35, 100